

A Framework for Diagnosis of Critical Faults in Unmanned Aerial Vehicles

Søren Hansen* Mogens Blanke*,*** Jens Adrian**

* *Automation and Control Group, Dept. of Electrical Engineering, Technical University of Denmark (DTU), DK-2800 Lyngby, Denmark.*

** *Danish Forces Joint UAV Team, Naval Weapons School, DK-4583 Sjællands Odde, Denmark.*

*** *AMOS CoE, Institute of Technical Cybernetics, Norwegian Univ. of Science and Technology (NTNU), NO-7491 Trondheim, Norway.
(E-mail: sh@elektro.dtu.dk, mb@elektro.dtu.dk)*

Abstract: Unmanned Aerial Vehicles (UAVs) need a large degree of tolerance towards faults. If not diagnosed and handled in time, many types of faults can have catastrophic consequences if they occur during flight. Prognosis of faults is also valuable and so is the ability to distinguish the severity of the different faults in terms of both consequences and the frequency with which they appear. In this paper flight data from a fleet of UAVs is analysed with respect to certain faults and their frequency of appearance. Data is taken from a group of UAV's of the same type but with small differences in weight and handling due to different types of payloads and engines used. Categories of critical faults, that could and have caused UAV crashes are analysed and requirements to diagnosis are formulated. Faults in air system sensors and in control surfaces are given special attention. In a stochastic framework, and based on a large number of data logged during flights, diagnostic methods are employed to diagnose faults and the performance of these fault detectors are evaluated against flight data. The paper demonstrates a significant potential for reducing the risk of unplanned loss of remotely piloted vehicles used by the Danish Navy for target practice.

1. INTRODUCTION

Fault Diagnosis (FD) and Fault Tolerant Control (FTC) are techniques that can strengthen safety-critical systems, such as controllers for Unmanned Aerial vehicles (UAV), and make them more reliable. A more reliable control system will of course produce a more beneficial and useful end product, in this case for the entire Unmanned Aircraft System (UAS). It is therefore important to include aspects of fault diagnosis when designing a system. However in some cases, for various reasons, this is not done. This paper explores the possibilities to add on a diagnosis framework to an existing UAS, where the aircraft do not have a build in FD/FTC systems. The system is tested against a couple of known faults that has occurred on these types of aircraft and where the existing controller reacted undesirable, but where information about the imminent fault was available in sensor data.

The literature on research aiming at improving overall safety and reliability of UAVs is quite rich. General treatments of the subject were covered by (Edwards et al., 2010) and (Zolghadri et al., 2013) highlighting some of the major advances within in recent years. A full treatment of how to accommodate to faults affecting the control of a UAS was shown in (Ducard and Geering, 2008) and (Ducard, 2009) where manoeuvrability was the main focus.

Specific faults related to aircraft have been studied extensively and partly reported in the open literature. For the case of control surface loss, estimation of the reduced

flight envelope and active FD was dealt with by (Bateman et al., 2011). In (Henry et al., 2012), methods using linear parameter varying methods were shown to be efficient for this problem. Research on the airspeed sensor related issues have been treated in (Samy et al., 2011) and (Wheeler et al., 2011) who analysed performance of linear time-invariant fault detection methods applied on parallel airspeed sensors.

This overview paper draws upon results from airspeed sensor system diagnosis (initial results in (Hansen et al., 2010) and a detailed scrutiny in (Hansen and Blanke, 2014)) and diagnosis of control surface defects (with different approaches presented in (Hansen and Blanke, 2012), (Hansen and Blanke, 2013) and (Blanke and Hansen, 2013)).

The paper is organised in five sections. Following this brief introduction a description of the diagnosis system is provided as well as a description of the UAS it is made for. After this a introduction to the types of faults considered within this system is given, which precedes an example of the diagnosis system and a conclusion.

2. BACKGROUND AND CONTEXT

The Danish Navy uses remotely operated drones for target practice and other tasks. These aircraft are constructed with aim at low complexity and low cost. They lack redundancy in sensors and actuators and the build in avionics is non-redundant as well. The type of drone dealt

with in this paper lands by parachute, hence the remedial action to critical faults will be an abortion of mission and release of the parachute. Graceful degradation is possible to a certain extent but need to be activated via telemetry: operator commands can reconfigure the onboard autopilot between a few predetermined modes and gains could be changed. However, time to react to critical faults is rather short, typically in the order seconds to minutes, so very clear diagnostic messages and decision support need be provided to an operator if he shall have a chance to react timely.

Systems that are constructed with fault tolerance in mind already from the design stage, would have a system and software architecture that enable diagnosis and fault accommodation. The means to do so are well known but have emerged only slowly in aerospace applications, see eg. (Bak et al., 1996) and (Goupil, 2010). With an air vehicle operator (AVO) in the loop, diagnosis need be timely and the ratio between detection and false alarm probability must be very high. Otherwise, the diagnostic system will soon loose credibility by the AVO's rendering the decision support useless.

The aim for the research collaboration described in this paper was hence,

- Make early warning possible from telemetry data.
- Make detection and false alarm probabilities essential design parameters.
- Use mainly data driven diagnosis as detailed modelling may not be an option.
- Ensure robustness to parameter changes due to loading etc.

The starting point for this diagnosis framework is a low-complexity UAV used for target practice which has the basic sensor suit consisting of IMU (Inertial Measurement Unit), airspeed sensor, height sensor and a GPS receiver. An onboard autopilot controls the aircraft to follow a route of waypoints send to it from a base station. The route can be changed online however the aircraft must at all time be within range of the base stations radio transmitter. More details about the UAS can be found in (Meggitt Defence Systems Ltd., 2008).

3. DIAGNOSIS SETUP DESCRIPTION

The suggested diagnosis system should attempt to diagnose certain critical faults using a low-complexity aircraft model and the available telemetry data, without adding any new hardware or modify the existing control system of the aircraft.

The general approach is shown in Fig. 1. Given the commands it is possible to calculate the expected behaviour of aircraft. By comparing this to the sensor values returned in the aircraft telemetry it is possible generate residual signals. Small variations in these residual signals can be used to tune the model parameters to better describe the specific aircraft and the influences of surrounding factors such as wind. A large variation on the residuals indicate a fault. The ability to distinguish variations due to disturbances from variations due to faults is critical for this setup. The Generalised Likelihood Ratio Test (GLRT) has been used for change detection, with good results. The

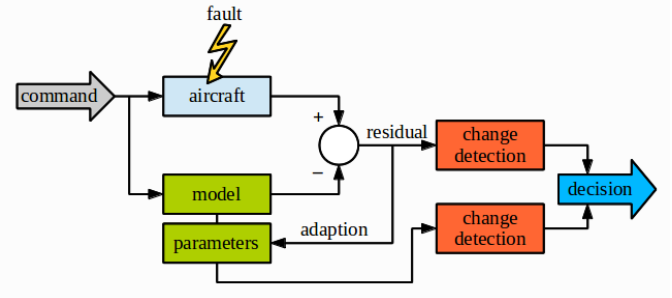


Fig. 1. Block diagram of the diagnosis setup.

GLRT is used to distinguish between the following two hypothesis about signal x at sample n .

$$\begin{aligned} \mathcal{H}_0 : x_n &= w_n \\ \mathcal{H}_1 : x_n &= A + w_n. \end{aligned} \quad (1)$$

The \mathcal{H}_0 hypothesis is the nominal case where the expected noise w is present. In the alternative \mathcal{H}_1 hypothesis the signal has been offset by a mean around 0 by some value A . If the difference between observations and the model are statistically significant within a desired false alarm probability P_F and detection probability P_D a fault hypothesis is confirmed. GLRT detectors are derived according to the observed distribution of residuals.

From Fig. 1 it is also realised that an effect of a fault will be present on the model parameters as a result of the adaptation feedback from the residual. Changes on the model parameters are therefore also monitored. A significant increase in the performance of the diagnosis system was achieved by combining both change detector outputs, utilising the joint distribution of test statistic for residuals and parameters, see (Blanke and Hansen, 2013) for details. It is noted that the parameter adaptation of the residual generator is stopped when residual's test statistic change. Otherwise faults would be masked and change detection using the strong detectability assumption of the model (1) could not be applied on residuals.

To distinguish between the hypotheses (1) the GLRT expresses a ratio between the two maximum likelihood estimates over a data window of size M given the residual $\mathbf{x}(i)$ and subject to the hypothesis,

$$S_j^k(\mathbf{x}, A) = \ln \sum_{i=k-M}^k \frac{p(\mathbf{x}(i); \mathcal{H}_1)}{p(\mathbf{x}(i); \mathcal{H}_0)} \quad (2)$$

The well-known GLRT test statics $g(k)$ for this model is obtained for a Gaussian, IID signal $x(i)$ as

$$g(k) = \max_{k-M \leq j \leq k} \max_A S_j^k(\mathbf{x}(i), A) \quad (3)$$

where j is the hypothetical instant when the change occurs. The decision \mathcal{H}_1 is taken if $g(k) > \gamma$ where A and the change instant are estimated by the GLRT. The threshold value γ is usually fixed or time-varying (adaptive), as used by (Verdier and Vila, 2008), but an obstacle is that theoretical calculation of γ requires the distribution of residuals to be known and the residual itself to be IID. An obstacle to residual evaluation is that residuals observed from numerous UAV flights show heavily correlation. The setup employed in this paper is therefore to estimate a

threshold from data: the distribution of test statistic is estimated and a threshold is calculated based on a required P_F . This approach was introduced in (Blanke et al., 2012) and further explored in (Galeazzi et al., 2013).

Fig. 2 shows the cumulative distribution function (CDF) for the test statistic ($g(k)$) of residuals for normal flights (\mathcal{H}_0). The dotted line in the probability plot is the estimated CDF for the distribution. A false alarm probability $P_F = 0.0005$ is obtained by selecting $\gamma = 50$ on the abscissa axis that corresponds to $1 - P_F = 0.9995$ on the ordinate axis. The test statistic is denoted T_L in the title fields of the plots.

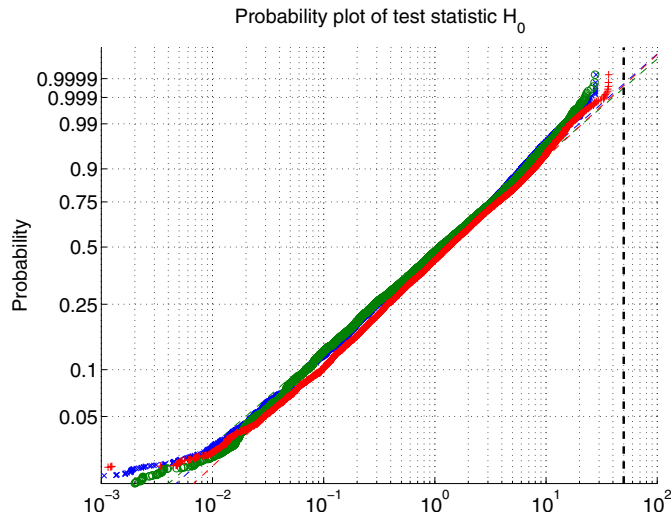


Fig. 2. Probability plot of three flights under \mathcal{H}_0 with detection threshold.

Fig. 3 shows the CDF of data during \mathcal{H}_1 for two different control surface faults. Case *I* is a low severity mechanical slip of an aileron actuator where the AVO should be warned about the fault but mission could be continued, however at higher risk. The low detection probability $P_F = 0.5$ would be an issue with this fault and supplementary information from parameter estimation could be beneficial. Case *II* is a high severity event giving loss of control of an aileron where early detection is essential to allow the AVO sufficient time to react to the event.

4. FAULT CATEGORIES INVESTIGATED

Within this framework, mainly two categories of faults has been investigated since data logs from several events of these types were available for analysis. The faults are: a) *airspeed system defects*, b) *control surface actuator or fin defects*. The defects are subdivided according to their severity: level *L* has low severity, aircraft flight envelope is not affected during normal manoeuvres; level *H* has high severity, aircraft flight envelope is affected during normal manoeuvres.

A summary of flight records available without any faults and with either of these types of defects are shown in Table 1. Both fault types has a course which makes them well suited for this kind of diagnosis in that they are visible in the telemetry data some time before aircraft control is lost, in case of severity level *H*, and for the remaining duration of flight in case of severity level *L*. This means

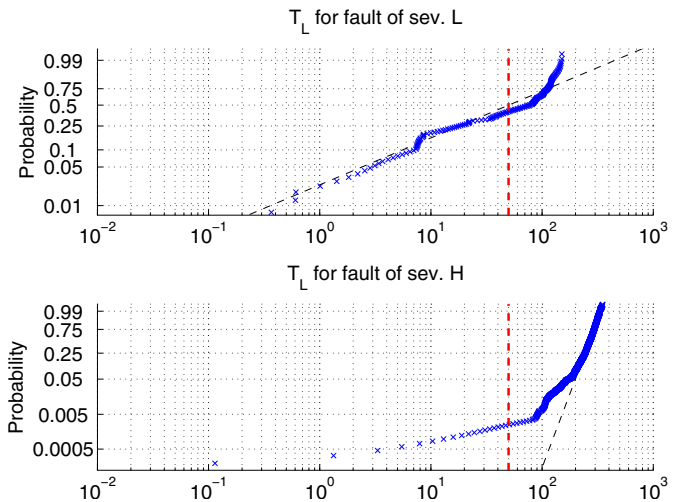


Fig. 3. Probability plot of the change detectors output for different faults.

Table 1. Flight time records under not normal conditions and all analysed flights

	time with fault	time span analysed
airspeed sensor	234 s	1500 min
control surface (sev. <i>L</i>)	9534 s	1250 min
control surface (sev. <i>H</i>)	42 s	1250 min

that a certain reaction time is available for the AVO to react to a timely warning about a defect diagnosed.

It is important to note that one cannot draw any conclusions on aircraft reliability based on the numbers in Table 1. This only shows the amount of data analysed during designs of the different parts of the diagnosis system. The amount of flight time with a fault is also limited for the level *H* faults, since these always leads to a crash fairly quickly after occurrence.

4.1 Airspeed System Defect

In order to measure the airspeed a pitot static system is often employed on aircraft. By measuring the pressure difference between two ports mounted on the body of the aircraft it is possible to measure the airspeed. This is an important measure since it enables the control system to keep the aircraft within its specified velocities and avoid stalls. The pitot static system used is very sensitive to clogging of the ventilation ports. Especially moist or dew on the aircraft tends to freeze up in higher altitudes and thereby clog the ports.

Fig. 4 shows data from an incident with icing of a pitot tube. The aircraft ground speed estimated by the GPS is plotted together with the airspeed indicated by the pitot static system. At approximately $t = 2140$ s the fault begins to be visible as a high increase in the ground speed compared to airspeed. The increase in speed is the autopilot responding to the decrease in measured airspeed as a result of the fault.

Using the measurements often available on this type of aircraft, namely, the airspeed measurement v_{pitot} , velocity measured by GPS and compensated for wind $v_{gps2air}$, and the expected velocity v_{thrust} obtained at a known engine

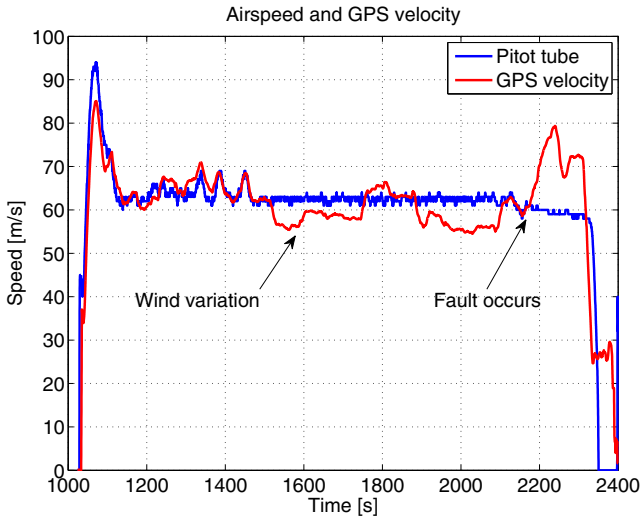


Fig. 4. Data from pitot tube and GPS velocity shown for a case where the pitot tube clogs.

shaft speed, it is possible to obtain a set of residuals describing the differences between these measurements. This gives rise to three residuals described by their parity relations shown in Table 2. In the table a "1" indicate that

Table 2. Parity relations.

Residual	v_{pitot}	$v_{gps2air}$	v_{thrust}
R_1	1	1	0
R_2	1	0	1
R_3	0	1	1

the current residual is depending on this variable. This means that a fault occurring on v_{pitot} will affect residual R_1 and R_2 , but not R_3 . The possibility of isolating a fault is evident for cases of single faults. Isolation if multiple faults should occur could be accomplished using active fault isolation techniques (Poulsen and Niemann, 2008), (Gelso and Blanke, 2009). The remedial action in case of an airspeed sensor system fault would be to avoid using airspeed in the avionics. This is an option in the particular system that can be activated by the AVO.

The estimates of airspeed are obtained in different ways each of which require that solutions to specific issues are obtained. The main obstacle in using the GPS velocity is to transform this into the frame of the airspeed. An estimate of the wind field is needed to make the connection.

To obtain this connection a simplified 2D perspective on the velocities is taken. The aircraft velocity relative to air \mathbf{v}_{rel} is related to the ground speed vector \mathbf{v}_g with this vector sum: $\mathbf{v}_g = \mathbf{v}_{rel} + \mathbf{v}_w$. The wind velocity vector, \mathbf{v}_w is defined such that it points in the direction the wind blow. The size of the airspeed can then be formulated using the standard cosine rule for triangles

$$v_{rel}^2 = v_w^2 + v_g^2 - 2v_g v_w \cos(\psi_w - \psi_g), \quad (4)$$

where the vectors are put into polar form. In this, ψ_w , is the wind angle and the heading of the aircraft is denoted ψ_g .

The airspeed measurement given by the pitot tube is offset by the aircraft angle of attack α and side slip β , in relation

to v_{rel} . Since measurements of α and β are not available the following simplified conversion is used:

$$v_{pitot} = \cos(\alpha) \cos(\beta) v_{rel} \simeq a v_{rel} \quad (5)$$

An Extended Kalman Filter (EKF) is now used to estimate $[v_w, \psi_w, a]^T$. These are modelled as random walk processes. By using the EKF estimates and combining (4) and (5) it is possible to generate a residual honouring the first row in Table 2.

$$R_1 = v_{pitot} - \hat{a} \sqrt{\hat{v}_w^2 + v_{gps}^2 - 2v_{gps} \hat{v}_w \cos(\hat{\psi}_w - \psi_{gps})} \quad (6)$$

The thrust based velocity v_{thrust} is generated using a model of the engine and propellers delivered thrust at certain throttle settings. The longitudinal dynamics can in general be described by:

$$m \dot{v}_{pitot} = m(rv - qw) + F_{Ax} - mg \sin(\theta) + F_T \quad (7)$$

with $[p, q, r]^T$ being the angular rates of the aircraft, θ the pitch angle, m the mass, F_T the thrust force and F_{Ax} the aerodynamic force in this axis. This is approximated by

$$F_{Ax} = \frac{1}{2} \rho S v_{pitot}^2 \Theta_{uu} = m F_1(v_{pitot}, t) \quad (8)$$

Using an observer v_{pitot} can be estimated using the dynamic equation and thereby the second residual of Table 2 is formed.

$$R_2 = v_{pitot} + \left(\int g \sin(\theta) - \frac{T_{nn} n^2 + T_{nu} n \hat{v}_{pitot}}{m} - F_1(\hat{v}_{pitot}, t) \hat{\Theta}_{uu} dt \right) - L(v_{pitot} - \hat{v}_{pitot}). \quad (9)$$

With n being the propeller angular velocity, T_{nn} and T_{nu} is thrust coefficient of the propeller, and L is the observer gain.

Following the voting scheme described in Table 2 the third residual is the difference between the two estimates of airspeed. Since both $v_{gps2air}$ and v_{thrust} relies on the airspeed measurement in their estimation procedures, it is impossible achieve independence of v_{pitot} . However, since the purpose of R_3 is to ensure isolability of the airspeed measurement fault, its value is only required when R_1 and/or R_2 indicate an alarm. With

$$R_3 = v_{gps2air} - v_{thrust} \quad (10)$$

and setting adaptation on hold when a fault is detected, R_3 can be used for isolation. If an airspeed fault is detected, v_{pitot} can not re-enter in calculations that estimate $v_{gps2air}$ and v_{thrust} . These estimates will therefore after a while become increasingly uncertain, which in turns affects R_3 . However, as long as R_3 's value is reliable up to and shortly after detection, it serves the purpose.

4.2 Control Surface or Actuator Defect

One of the most critical faults that can happen to an aircraft is partly or totally loss of one of the control surfaces. This reduces manoeuvrability of the aircraft significantly and will in most cases lead to a crash. This is a defect of high severity, denoted level H . Less critical faults include misalignment of the actuator to fin linkage and will mainly affect steady state trim and also the available range of control surface deflection, the latter due to mechanical limits. These are denoted severity level L .

Data logging from an incident with a type H fault is shown in Fig. 5. The figure shown the selected telemetry data

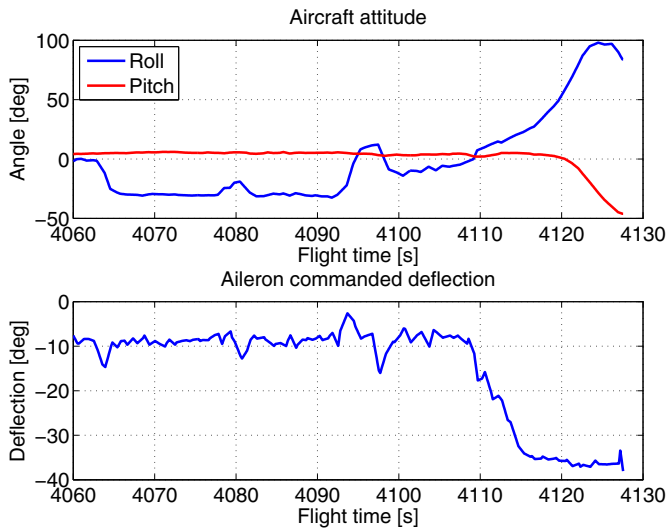


Fig. 5. Top: Roll and pitch signals. Bottom: Command signal to ailerons. An incident where control of an aileron is lost during flight.

for the aircraft up to and just after an incident happens to the aileron. Just before $t = 4110$ s the aircraft starts rolling right, even though the commanded signal is for a left roll. From this point on there is no relation between the commanded signal and the aircraft's manoeuvres. The aircraft crashed shortly after and the subsequent investigation determined that control of an aileron was lost during flight.

A system to diagnose this type of fault can be created using the dynamic models of the aircraft. Aircraft mathematical modelling requires a 6 degree of freedom model, where both dynamic and kinematic equations of motion are needed to characterise the aircraft, see eg. (Stevens and Lewis, 2003). Utilising this model implies detailed knowledge about the aerodynamic coefficients and this information is not always available for the cheaper UAV's. For control surface fault diagnosis the important feature is the relationship between surface deflection and angular rates of the aircraft.

Earlier studies investigated how dynamic and semi-static models could be used for diagnosis of control surface faults on this family of aircraft (Hansen and Blanke, 2012) and the issue has been dealt with for large aircraft with hydraulic actuators in (Varga, 2010). For small aircraft with uncertain or lacking model information, an adaptive and very simple model of this relationship was found useful (Blanke and Hansen, 2013). The following three relations for roll rate (p), pitch rate (q) and yaw rate (r), calculated at sample k , are related to the commanded deflections to aileron δ_a and elevator δ_e as,

$$p[k] = a_{pa}\delta_a[k] + b_{pa} \quad (11)$$

$$q[k] = a_{qe}\delta_e[k] + b_{qe} \quad (12)$$

$$r[k] = a_{ra}\delta_a[k] + b_{ra}r[k-1] + c_{ra}, \quad (13)$$

where b_{pa} , b_{qe} and c_{ra} are bias terms and a_{pa} , a_{qe} and a_{ra} are gain factors. Equation (13) includes the integrating

effect between the aileron and yaw rate in the b_{ra} term. This approach separates the lateral and longitudinal states since the aileron is only related to roll and yaw and the elevator only to pitch. Neglecting essential dynamics of the aircraft, and couplings between some motions, this model is indeed over-simplified with respect to describe dynamic behaviours. However, as will be shown, the model is sufficient and effective for fault diagnosis when means are taken to make change detection robust to both unmodelled dynamics and to natural parameter variations.

Each of the parameters in equations (11) - (13) must be determined to fit the aircraft response to get the best result of the diagnosis as possible. From the block diagram of Fig. 1 it is seen that the parameters are adapted during flight such that small deviations from aircraft to aircraft are removed. The equations are on a form of an ARX function and hence a Recursive Least Squares (RLS) filter, as the following, can be used to estimate the parameters.

$$\varepsilon[k] = y[k] - \varphi[k]^T \hat{\Theta}[k-1] \quad (14)$$

$$P[k] = \left(\lambda_f P[k-1]^{-1} + \varphi[k] \varphi[k]^T \right)^{-1} \quad (15)$$

$$\hat{\Theta}[k] = \hat{\Theta}[k-1] + P[k] \varphi[k] \varepsilon[k]. \quad (16)$$

In this, λ_f is the forgetting factor and $P[k]$ is the covariance. The initial value of $P[k]$ can be determined from some average of test flights: running the estimator for data from steady wings-level flight without faults would give an a-priori value of $P[k]$. The forgetting factor is tunable and this is one of the parameters to be considered when combining parameter identification with residual evaluation for diagnosis. Control surface defects will give rise to rapid change in the input/output signals and hence in the prediction error (14) and subsequently appear as a parameter adaptation to the faulty case.

5. DIAGNOSIS EXAMPLE

This section shows a brief example to illustrate the diagnosis system properties for a case of a control surface fault of severity L .

The first step in a diagnostic procedure is always to ensure that false alarms are not triggered during normal conditions. To validate this, Fig. 2 showed a probability plot of the test statistic from the GLRT test on residuals with no faults occurring. The fault incidence considered here is that one of the servos controlling an aileron flap slips in the teeth of the cogwheel that connects the servo with the fin. Data from two of the residuals are shown in Fig. 6. A shaded (yellow) area in Figure 6 illustrates where the fault occurs, the actual onset is believed to be where sudden fluctuations occur in the residual, or slightly previous to this. The fault is not critical for the continues flight and therefore of severity L according to Table 1. This is hence a case where post flight maintenance is the focus and time to detect is not a key point. The detection of the fault is delayed 20 s from its occurrence due to effects of the windowing in the change detectors.

The vertical black line indicates the detector threshold of 50 and test statistic values above this threshold will trigger the \mathcal{H}_1 hypothesis. Data points for the entire shaded area of Fig. 6 are plotted. The probability plot in Fig 7 shows

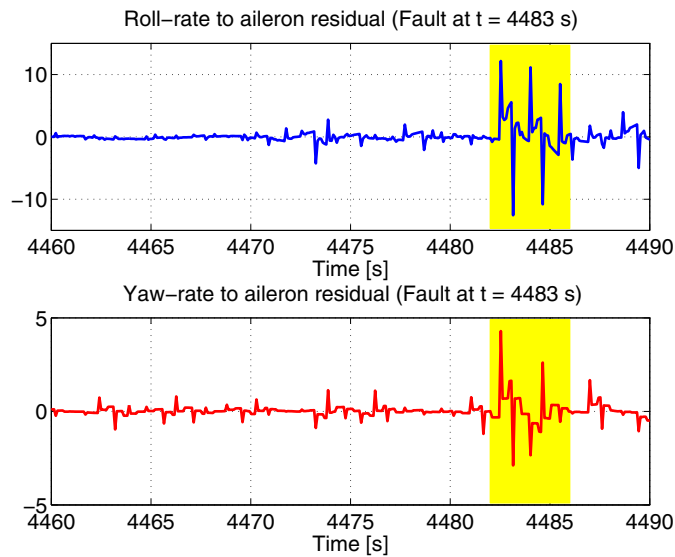


Fig. 6. Residuals for a servo fault of low severity. The fault occurs in the beginning of the shaded area and remains.

that around 10% of the time series data are above the threshold level. This indicates that if the threshold is based solely on change in test statistics of the residual, the threshold should be increased by a factor 5 to obtain a false alarm probability below 0.05%. When a combined threshold of parameter change and test statistics of the residual are used for hypothesis testing, the threshold of the latter can be lowered to obtain higher detection performance.

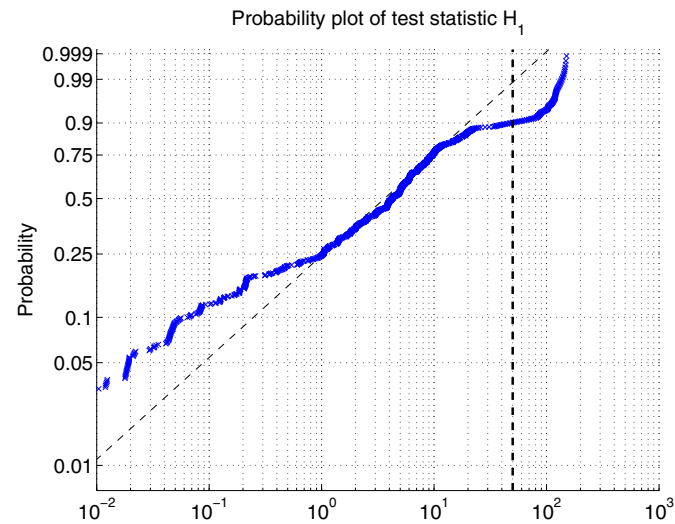


Fig. 7. Probability plot of test statistic data for the flight when under \mathcal{H}_1 in the case of the low severity fault. Detection threshold is shown as the vertical dotted line.

Fig. 8 shows a scatter diagram of the change detector output and two parameters of Eq. (13). This illustrates that a change happens in estimated parameter values for this particular fault that has low severity. The test statistics of the residual-based change detector reacts late on the change, and the low severity fault is captured by the change in parameter values.

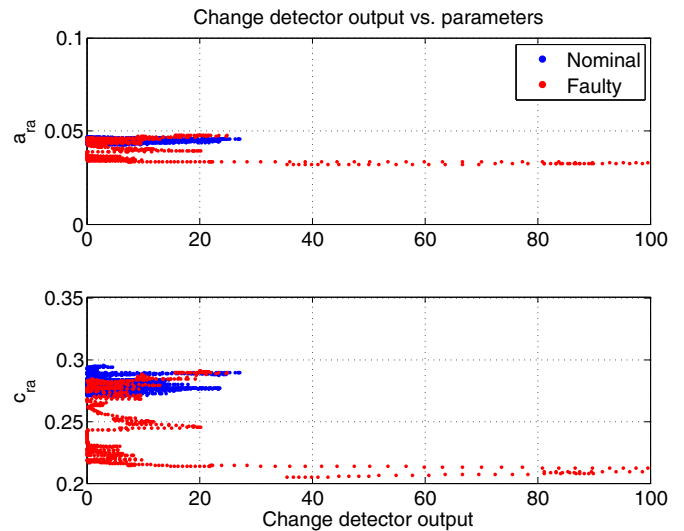


Fig. 8. Scatter plot of the residuals change detector output and the model parameters in case of a fault of low severity.

Fig. 9 shows a scatter diagram of the change detector output and the two parameters when a fault of high severity occurs. The residual-based change detector shows a large response in test statistic when the fault occurs.

The incidents illustrate that by combining hypothesis testing of parameter changes with change in test statistics of the residuals, a better detection performance is obtained in comparison with applying change detectors to the individual quantities.

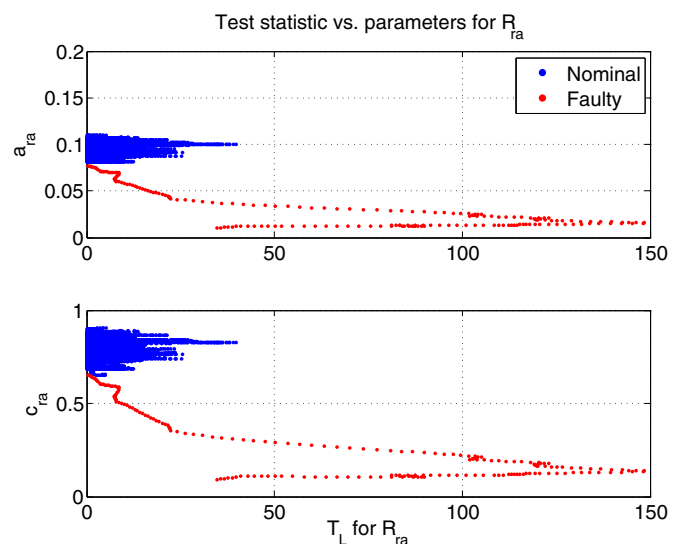


Fig. 9. Scatter plot of the residuals change detector output and the model parameters in case of a fault of high severity.

Use of combined parameter and test statistic change detection gave fault isolation with very favorable detection and false alarm probabilities, and also rapid detection in cases of type H faults on control surfaces (Blanke and Hansen, 2013). The case presented here illustrates that the type L fault is best detected by a parameter estimating

scheme, but that the combined approach captures the fault irrespective of its severity.

6. CONCLUSION

This paper has given an overview of a fault diagnosis system designed specifically to diagnose two high severity types of faults for a UAV. The diagnosis approach assumed that only basic system knowledge and standard UAV sensors were available. We employed self-tuning methods to generate models for diagnosis. Diagnosis was designed to work on telemetry data from the aircraft. Examples of the capabilities of the diagnostic were demonstrated. High severity faults were detected rapidly and, in the cases investigated, timely enough to avoid a failure of mission. Low severity events were diagnosed with low probability of false alarm. Further improvement is envisaged to be obtainable from exploitation of the joint probability between parameter estimates and residual test statistic.

ACKNOWLEDGEMENTS

The support from the Danish Forces Joint UAV Team in conducting experiments is greatly appreciated. The authors also wish to acknowledge the collaboration with Meggitt Defence Systems, UK, for providing access to telemetry data protocols for their systems.

REFERENCES

- Bak, T., Wisniewski, R., and Blanke, M. (1996). Autonomous attitude determination and control system for the Ørsted satellite. In *Proc. 1996 IEEE Aerospace Applications Conference*.
- Bateman, F., Noura, H., and Ouladsine, M. (2011). Fault diagnosis and fault-tolerant control strategy for the aerosonde uav. *IEEE Trans. on Aerospace and Electronic Systems*, 47 (3), 2119–2137.
- Blanke, M., Fang, S., Galeazzi, R., and Leira, B.J. (2012). Statistical change detection for diagnosis of buoyancy element defects on moored floating vessels. In *Proc. IFAC SAFEPROCESS*, 462–467.
- Blanke, M. and Hansen, S. (2013). Towards self-tuning residual generators for uav control surface fault diagnosis. In *Proc. 2nd International Conference on Control and Fault-Tolerant Systems*, 37–42.
- Ducard, G. and Geering, H.P. (2008). Efficient nonlinear actuator fault detection and isolation system for unmanned aerial vehicles. *Journal of Guidance, Control, and Dynamics*, 31 (1), 225–237. doi:10.2514/1.31693.
- Ducard, G.J.J. (2009). *Fault-tolerant Flight Control and Guidance Systems*. Springer Verlag.
- Edwards, C., Lombaerts, T.J.J., and Smaili, M.H. (eds.) (2010). *Fault Tolerant Flight Control: A Benchmark Challenge*. Springer.
- Galeazzi, R., Blanke, M., and Poulsen, N.K. (2013). Early detection of parametric roll resonance on container ships. *IEEE Transactions on Control Systems Technology*, 21(2), 489–503. doi:10.1109/TCST.2012.2189399.
- Gelso, E.R. and Blanke, M. (2009). Structural analysis extended with active fault isolation -methods and algorithms. In *Proc. 7th IFAC Symposium on Fault Detection, Supervision and Safety of Technical Processes*, 597–602. doi:10.3182/20090630-4-ES-2003.0009.
- Goupil, P. (2010). Oscillatory failure case detection in the a380 electrical flight control system by analytical redundancy. *Control Engineering Practice*, 18, 1110 – 1119.
- Hansen, S. and Blanke, M. (2012). In-flight fault diagnosis for autonomous aircraft via low-rate telemetry channel. In *IFAC International Symposium on Fault Detection, Supervision and Safety for Technical Processes*.
- Hansen, S. and Blanke, M. (2013). Control surface fault diagnosis with specified detection probability - real event experiences. In *2013 International Conference on Unmanned Aircraft Systems*.
- Hansen, S. and Blanke, M. (2014). Diagnosis of airspeed measurement faults for unmanned aerial vehicles. *IEEE Trans. Aerospace and Electronic Systems*, 50 (1).
- Hansen, S., Blanke, M., and Adrian, J. (2010). Diagnosis of uav pitot tube defects using statistical change detection. In *7th Symposium on Intelligent Autonomous Vehicles*.
- Henry, D., Zolghadri, A., Cieslak, J., and Efimov, D.V. (2012). A lpv approach for early fault detection in aircraft control surfaces servo-loops. In *IFAC Proceedings IFAC SAFEPROCESS'2012*, 806 – 811. Mexico City. doi:10.3182/20120829-3-MX-2028.00047.
- Meggitt Defence Systems Ltd. (2008). Banshee aerial target system. URL http://www.meggittdefenceuk.com/PDF/Banshee_aerial_target_system.pdf.
- Poulsen, N.K. and Niemann, H. (2008). Active fault diagnosis based on stochastic tests. *International Journal of Applied Mathematics and Computer Science*, 18 (4), 487–496.
- Samy, I., Postlethwaite, I., and Gu, D.W. (2011). Unmanned air vehicle air data estimation using a matrix of pressure sensors: a comparison of neural networks and look-up tables. *Journal of Aerospace Engineering*, 225 (7), 807–820.
- Stevens, B.L. and Lewis, F.L. (2003). *Aircraft Control and Simulation*. John Wiley & Sons, 2nd edition.
- Varga, A. (2010). Detection and isolation of actuator/surface faults for a large transport aircraft. *Lecture Notes in Control and Information Sciences*, 399, 423–448.
- Verdier, G. and Vila, N.H.A.J.P. (2008). Adaptive threshold computation for cusum-type procedures in change detection and isolation problems. *Computational Statistics and Data Analysis*, 52, 4161–4174.
- Wheeler, T.J., Seiler, P., Packard, A.K., and Balas, G.J. (2011). Performance analysis of fault detection systems based on analytically redundant linear time-invariant dynamics. In *Proc. 2011 American Control Conference (ACC 2011)*, 214–219.
- Zolghadri, A., Henry, D., Cieslak, J., Efimov, D., and Goupil, P. (2013). *Fault Diagnosis and Fault-Tolerant Control and Guidance for Aerospace Vehicles - From Theory to Application*. Springer.